PAPER

Spinons and holons with polarized photons in a nonlinear waveguide

To cite this article: Ming-Xia Huo *et al* 2012 *New J. Phys.* **14** 075027

View the article online for updates and enhancements.

Spinons and holons with polarized photons in a nonlinear waveguide

Ming-Xia Huo[1]**, Dimitris G Angelakis**[1,2,4]
and Leong Chuan Kwek[1,3]

[1] Centre for Quantum Technologies, National University of Singapore,
3 Science Drive 2, Singapore 117542, Singapore
[2] Science Department, Technical University of Crete, Chania, Crete, Greece
[3] National Institute of Education and Institute of Advanced Studies,
Nanyang Technological University, 1 Nanyang Walk, Singapore 637616,
Singapore
E-mail: dimitris.angelakis@gmail.org

Abstract. We show that the spin–charge separation predicted for correlated fermions in one dimension could be observed using polarized photons propagating in a nonlinear optical waveguide. Using coherent control techniques and employing a cold atom ensemble interacting with the photons, large nonlinearities in the single-photon level can be achieved. We show that the latter can allow for the simulation of a strongly interacting gas, which is made of stationary dark-state polaritons of two species and is shown to form a Luttinger liquid of effective fermions for the right regime of interactions. The system can be tuned optically to the relevant regime where the spin–charge separation is expected to occur. The characteristic features of the separation as demonstrated in different spin and charge densities and velocities can be efficiently detected via optical measurements of the emitted photons with current optical technologies.

IOP Institute of Physics   **Φ** DEUTSCHE PHYSIKALISCHE GESELLSCHAFT

Contents

1. Introduction

1.1. Spin–charge separation and quantum simulators

One-dimensional (1D) physical systems have attracted much attention owing to their novel and sometimes spectacular features. Unlike 2D or 3D systems, the physics of the 1D Lieb–Liniger model [1] is captured well by the Luttinger liquid theory in the low-energy domain [2]. In the 1D Luttinger liquid theory, collective excitations rather than single excitations appear owing to the tight transverse confinement forcing particles to move along one direction and thus converting any individual motion into a collective one. The collective modes of the spin and the charge in 1D electronic gases surprisingly can be shown to propagate with different velocities, i.e. the spin and the charge separate into spinons and holons [2–5]. In experiments, the observation of spin–charge separation is, however, challenging—the control of interactions is still elusive and no distinct features of separation are obtained, although several seminal works have been done using copper oxide chain compounds $SrCuO_2$ [6], metallic chains [7], superconductors [8] and, more recently, GaAs/AlGaAs heterostructures [9–11].

Besides this, works on artificially engineered quantum optical systems in which many-body effects can be reproduced in well-controlled environments have emerged in recent years. To observe spin–charge separation in cold atoms, experimental proposals involving bosonic and fermionic species have been suggested [12–15]. However, the challenges in the trapping and cooling of fermionic gases, especially the lack of necessary individual accessibility and measurement of correlations in general, render current results inconclusive. Strongly correlated photons and polaritons, as hybrid light–matter quantum simulators, have recently been proposed. Initially using coupled resonator implementations [16], Mott transitions [17–19] and then effective spin models and fractional Hall states of light were shown to be possible [20–25]. More recently, by employing hollow-core optical waveguides filled with cold atom ensembles and using slow-light techniques [26–28], it was shown that it is possible to prepare a Tonks gas of photons [29]. Using two atomic species, a two-component Lieb–Liniger model has also been suggested recently [30]. Compared to cold-atom proposals, photonic proposals should allow for more direct measurements of local observables and correlation functions of the emitted photon states.

In this paper, we consider a novel scheme involving two oppositely circularly polarized quantum beams and single atomic species to simulate a two-component interacting gas in one dimension. We note the difference from an earlier scheme, where two quantum fields with different frequencies interacting with two species of four-level atoms were employed [30]. The present proposal has a distinct advantage in two major ways: firstly, in terms of more efficient detection of the correlation in output polarized states, and secondly, in terms of the loading and preparation process into the fiber which requires the handling of a single atomic species rather than two.

The paper is organized as follows. First we review the basics of the single- and two-component bosonic Lieb–Liniger model [1] and especially its mapping to the Luttinger liquid theory. We then describe in detail the preparation of a polaritonic Lieb–Liniger model with two bosonic components in the waveguide employing slow-light techniques. Finally, we discuss the range of optical parameters necessary to drive the system to the relevant spin–charge separation regime. We conclude by analyzing how the effective photonic spin and charge densities and velocities can be probed. This is done by releasing the trapped polaritons into outgoing photons where optical measurements can reconstruct the characteristic functions of the effect.

1.2. From Lieb–Liniger bosons to Luttinger liquids: the basics of spin–charge separation revisited

One of the most famous 1D models is the Lieb–Liniger model [1], which describes N bosons with a Dirac-delta interaction as

$$H^{\mathrm{s}} = -\frac{1}{2m} \sum_{i=1}^{N} \frac{\partial^2}{\partial z_i^2} + g \sum_{i<j=1}^{N} \delta\left(z_i - z_j\right),$$ (1)

where m is the mass and g is the interaction strength. Although the Lieb–Liniger model is exactly solvable through the Bethe ansatz approach, it is still generally very difficult to extract correlation functions from the solutions at any interaction regime. The Luttinger liquid theory, on the other hand, can give the low-energy universal description of the Lieb–Liniger model at low temperatures. In the Luttinger liquid phase, the low-energy excitations are no longer single but collective modes with linear dispersion. The confinement of interactions between particles in one dimension forces any individual motion to affect the collective system. A description of the dynamics in terms of collective bosonic fields is called the 'bosonization' approach and we present it briefly in the following.

Assume N particles described by $\psi(\mathbf{r}) = \psi(z)\varphi_0(\mathbf{r}_\perp)$, where the particles move along one direction, say the z-direction. Strong confinement is applied to the transverse direction $\mathbf{r}_\perp = \{x, y\}$, allowing only for the lowest-energy transverse quantum state $\varphi_0(\mathbf{r}_\perp)$ to be considered. The Lieb–Liniger model of the parallel component reads [2–5]

$$H^{\mathrm{s}} = \int \mathrm{d}z \left[\frac{1}{2m} \partial_z \psi^\dagger(z)\, \partial_z \psi(z) + \frac{g}{2} \rho^2(z) \right],$$ (2)

where the collective bosonic fields $\psi(z)$ and $\psi^\dagger(z)$ can be expressed as

$$\psi(z) = \mathrm{e}^{-\mathrm{i}\theta(z)} [\rho(z)]^{1/2}, \qquad \psi^\dagger(z) = [\rho(z)]^{1/2}\, \mathrm{e}^{\mathrm{i}\theta(z)},$$ (3)

with $\rho(z) = \psi^\dagger\psi$ the particle density and $\theta(z)$ the phase operator. As described in [2], the phase and density fields are canonically conjugated fields,

$$[\rho(z), \mathrm{e}^{\mathrm{i}\theta(z')}] = \delta(z - z')\mathrm{e}^{\mathrm{i}\theta(z')},$$ (4)

and the collective density operator can be expressed as

$$\rho(z) = \left[\rho_0 + \frac{1}{\pi}\partial_z\phi(z)\right] \sum_{m=-\infty}^{+\infty} \exp\{im[2\pi\rho_0 z + 2\phi(z)]\}. \tag{5}$$

If $\rho(z)$ varies slowly with z, we can retain the lowest-frequency component for $m = 0$ and write

$$\rho(z) \simeq \rho_0 + \frac{1}{\pi}\partial_z\phi(z), \tag{6}$$

where the fields $\theta(z)$ and $\frac{1}{\pi}\partial_z\phi(z')$ are canonically conjugated.

The Lieb–Liniger Hamiltonian (2) for the lowest component $\psi(z) \simeq e^{-i\theta(z)}\rho_0^{1/2}$ can be mapped to a Luttinger liquid with Hamiltonian (see [2–5]) the

$$H^{\rm s} = \int \frac{{\rm d}z}{2\pi}\left[\upsilon K^{\rm sl}(\partial_z\theta)^2 + \frac{\upsilon}{K^{\rm sl}}(\partial_z\phi)^2\right], \tag{7}$$

where all the interaction effects are encoded into two effective parameters: the propagation velocity of density disturbances υ and the so-called Luttinger parameter $K^{\rm sl}$ controlling the long-distance decay of correlations.

Going beyond the simple case with a single-component bosonic system, interesting physics can be obtained by mixing two bosonic components or by considering two internal degrees of freedom of bosons, which is analogous to assigning a 'spin' 1/2 to bosons. The two-component Lieb–Liniger model in this case would read

$$H^{\rm t} = \int {\rm d}z \sum_{s=\uparrow,\downarrow}\left[\frac{1}{2m_s}\partial_z\psi_s^\dagger(z)\partial_z\psi_s(z) + \frac{\chi_s}{2}\rho_s^2(z)\right] + \int {\rm d}z\chi_{\uparrow\downarrow}\rho_\uparrow(z)\rho_\downarrow(z), \tag{8}$$

where m_s is the mass and χ_s and $\chi_{\uparrow\downarrow}$ are the intra- and interspecies interactions with $s = \uparrow$, $\downarrow$ representing the two spins. Following the literature [2–5], the charge- and spin-related fields can be defined as

$$\theta_{\rm charge} = \frac{\theta_\uparrow + \theta_\downarrow}{\sqrt{2}}, \quad \theta_{\rm spin} = \frac{\theta_\uparrow - \theta_\downarrow}{\sqrt{2}}, \quad \phi_{\rm charge} = \frac{\phi_\uparrow + \phi_\downarrow}{\sqrt{2}}, \quad \phi_{\rm spin} = \frac{\phi_\uparrow - \phi_\downarrow}{\sqrt{2}}. \tag{9}$$

The Hamiltonian is divided into two parts (for more details see [2]) and reads as $H^{\rm t} = H_{\rm charge} + H_{\rm spin}$. The charge part is given by

$$H_{\rm charge} = \int \frac{{\rm d}z}{2\pi}\left[u_{\rm charge}K_{\rm charge}(\partial_x\theta_{\rm charge})^2 + \frac{u_{\rm charge}}{K_{\rm charge}}(\partial_x\phi_{\rm charge})^2\right], \tag{10}$$

and the spin part is defined as

$$H_{\rm spin} = \int \frac{{\rm d}z}{2\pi}\left[u_{\rm spin}K_{\rm spin}(\partial_x\theta_{\rm spin})^2 + \frac{u_{\rm spin}}{K_{\rm spin}}(\partial_x\phi_{\rm spin})^2\right] + 2\chi_{\uparrow\downarrow}\rho_0^2\cos\left(\sqrt{8}\phi_{\rm spin}\right) \tag{11}$$

under the separation conditions

$$\chi_\uparrow = \chi_\downarrow, \frac{\rho_{0,\uparrow}}{m_\uparrow} = \frac{\rho_{0,\downarrow}}{m_\downarrow}. \tag{12}$$

Here $\rho_0 = \rho_{0,\uparrow} + \rho_{0,\downarrow}$ and $\rho_{0,s}$ are the densities for two species. With $\chi = \chi_s$, $u = u_s = \sqrt{\rho_{0,s}\chi_s/m_s}$ and $K = K_s = \sqrt{\pi^2\rho_{0,s}/(m_s\chi_s)}$, the charge and spin velocities and Luttinger parameters are $u_{\rm charge,spin} = u\sqrt{1 \pm \chi_{\uparrow\downarrow}/\chi}$, $K_{\rm charge,spin} = K/\sqrt{1 \pm \chi_{\uparrow\downarrow}/\chi}$.
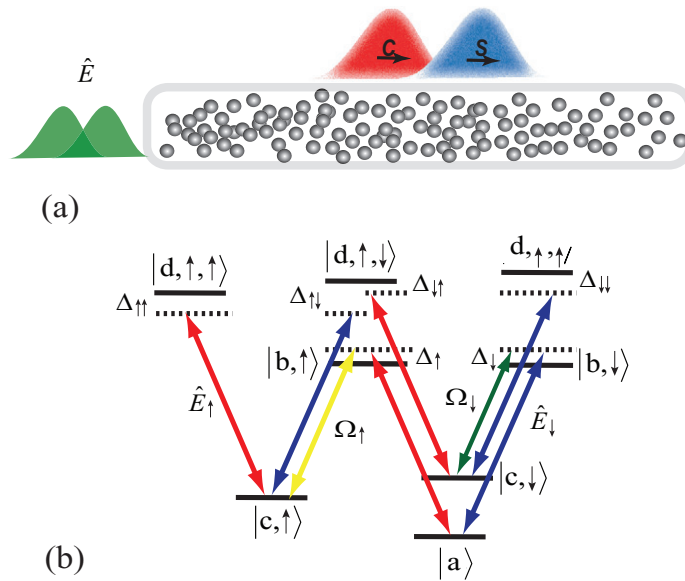
Figure 1. The model setup under consideration. In a nonlinear fiber (a hollow core version is shown here but a tapered fiber approach could also be used), the cold atoms are interacting with two quantum light fields $\hat{E}_s$ (red and blue arrowlines) and two pairs of classical fields $\Omega_{s,\pm}$ (yellow and green arrowlines), where $\pm$ denotes the forward or backward propagation direction. The atomic level diagram studied and possible atomic transitions driven by two oppositely circularly polarized quantum pulses $\hat{E}_s$ and two control beams Ω_s are shown in (b). Appropriately tuning the couplings of light fields to the corresponding atomic transitions forces the trapped polaritons to behave like an effective 1D quantum Luttinger liquid and reach the spin–charge separation regime. Coherently transferring the polaritons' correlations to propagating light pulses and allowing them to exit the fiber provides for efficient measurement of both the dynamics of propagation of effective spin and charge quasi-particles and the effective spin and charge velocities characteristic of the effect taking place.

2. Photonic spin–charge separation in nonlinear optical waveguides

2.1. The optical waveguide setup

Our proposal is based on exploiting the available huge photonic nonlinearities capable of being generated in specific quantum optical setups. More specifically, we envisage the use of a highly nonlinear waveguide where the necessary nonlinearity will emerge through the strong interaction of the propagating photons with existing emitters in the waveguide. Recent experiments have developed two similar setups in this direction, both capable of implementing our proposal with either current or near-future platforms. In these experiments, cold atomic ensembles are brought close to the surface of a tapered fiber [31, 32] or are loaded inside the core of a hollow-core waveguide [33–36] as shown in figure 1(a). The available optical nonlinearity based on the electromagnetically induced transparency effect can be used, as we will show, to create situations where the trapped photons obey Lieb–Liniger physics.

The process for generating the strongly correlated states of photons is as follows: first, laser-cooled atoms exhibiting a multiple atomic-level structure shown in figure 1(b) are moved into position so they will interact strongly with incident quantum light fields. Initially, resonant with the corresponding transitions, two optical pulses with opposite polarizations $\hat{E}_{\uparrow,+}(z,t)$ and $\hat{E}_{\downarrow,+}(z,t)$ are sent in from one direction, say the left side. They are injected into the waveguide with the co-propagating classical control fields $\Omega_{\uparrow,+}(t)$ and $\Omega_{\downarrow,+}(t)$ initially turned on. As soon as the two quantum pulses completely enter into the waveguide, the classical fields $\Omega_{s,+}$ are adiabatically turned off, converting $\hat{E}_{s,+}$ into coherent atomic excitations as in usual slow-light experiments for $s = \uparrow, \downarrow$. We then adiabatically switch on both $\Omega_{s,+}$ and $\Omega_{s,-}$ from the two sides. The probe pulses become trapped due to the effective Bragg scattering from the stationary classical waves as analyzed in [26–28]. At this stage the pulses are noninteracting with the photons expanding freely due to the dispersion. By slowly shifting the d-levels, the effective masses can be kept constant, whereas the effective intra- and interspecies repulsions are increased. This drives the system into a strongly interacting regime. This dynamic evolution is possible by keeping, for example, the corresponding photon detunings Δ_s constant while shifting the d-level. Once this correlated state is achieved, the fields—for example, $\Omega_{s,+}$—from the pair of control fields that trap polaritons are slowly turned off. This will release the corresponding quasi-particles by turning them into propagating photons, which will then exit the fiber. As all correlations established in the previous step are retained, these wave packets are comprised of two separate effective charge and spin density waves.

2.2. Realizing a two-component Lieb–Liniger model of polarized photons

The system described above and shown in figure 1 obeys the Hamiltonian

$$H^{\circ} = -\int \sum_s n_z^s \mathrm{d}z \left\{ -\Delta_s \sigma_{b,s;b,s} - \sum_{s'} \Delta_{ss'} \sigma^x_{d,s,s';d,s,s'} + \sqrt{2\pi}\left(g_s \sigma_{b,s;a} + \sum_{s'} g_{ss'} \sigma_{d,s,s';c,s'}\right) \right.$$

$$\left. \times \left(\hat{E}_{s,+}\mathrm{e}^{\mathrm{i}k_{Q,s}z} + \hat{E}_{s,-}\mathrm{e}^{-\mathrm{i}k_{Q,s}z}\right) + \left(\Omega_{s,+}\mathrm{e}^{\mathrm{i}k_{C,s}z} + \Omega_{s,-}\mathrm{e}^{-\mathrm{i}k_{C,s}z}\right)\sigma_{c,s;b,s} + \mathrm{h.c.} \right\}, \qquad (13)$$

where $s, s' = \uparrow, \downarrow$ and $|d, \uparrow, \downarrow\rangle = |d, \downarrow, \uparrow\rangle$. The continuous collective atomic spin operators $\sigma_{\mu;\nu} \equiv \sigma_{\mu;\nu}(z,t)$ describe the averages of the flip operators $|\mu\rangle\langle\nu|$ over atoms in a small region around z. The density of atoms is n_z^s and g_s, $g_{ss'}$ are the coupling strengths between the quantum fields and atoms, while Δ_s and $\Delta_{ss'}$ are one-photon detunings from the corresponding transitions. For simplicity, we assume that $g_s = g_{ss'} = g$. Furthermore, we label the two quantum and two classical fields with frequencies $\omega_{Q,s}$ and $\omega_{C,s}$ and wave vectors $k_{Q,s}$ and $k_{C,s}$, respectively. Both quantum fields $\hat{E}_{\uparrow,+}(z,t)$ and $\hat{E}_{\downarrow,+}(z,t)$ drive four possible atomic transitions. The fields $\hat{E}_{s,\pm}(z,t)$ are detuned by Δ_s from the transition $|a\rangle \to |b, s\rangle$ and by Δ_{ss} from $|c, s\rangle \to |d, s, s\rangle$. $\hat{E}_{s,\pm}(z,t)$ also drive the transitions from $|c, s\rangle \to |d, s, \bar{s}\rangle$ with detuning $\Delta_{s\bar{s}}$. Here $\bar{s} = \uparrow, \downarrow$ and $\bar{s} \neq s$. Finally, the applied classical control beams with Rabi frequencies $\Omega_{s,\pm}(t)$ couple to both atoms and drive the transitions $|b, s\rangle \to |c, s\rangle$.

The evolution of the slowly varying quantum operators $\hat{E}_{s,\pm}$ is given by four Maxwell–Bloch (MB) equations

$$(\partial_t + \nu\partial_z)\,\hat{E}_{s,\pm} = \mathrm{i}\sqrt{2\pi}\,n_z^s g\,(\sigma_{a;b,s,\pm} + \sigma_{c,s;d,s,s,\pm} + \sigma_{c,\bar{s};d,s,\bar{s},\pm}) \qquad (14)$$

with the four levels of the sth atoms denoted by $|a, s\rangle$, $|b, s\rangle$, $|c, s\rangle$ and $|d, s, s\rangle$. When writing down the MB equations (14), we have introduced the slowly varying collective operators

$$\sigma_{\mu;\nu} = \sigma_{\mu;\nu,+}(z, t)e^{ik_{Q,s}z} + \sigma_{\mu;\nu,-}(z, t)e^{-ik_{Q,s}z}, \tag{15}$$

and ν is the velocity of quantum fields in an empty waveguide[5]. In the derivation of equations of motion we assume the Rabi frequencies of the control fields to be slowly varied. The slow-light polariton operators are defined as

$$\Psi_{s,\pm} = \cos\theta_s \hat{E}_{s,\pm} - \sin\theta_s \sqrt{2\pi n_z^s}\sigma_{c,s;a}, \tag{16}$$

where $\tan\theta_s = g\sqrt{2\pi n_z^s}/\Omega_s$. For stationary polaritons we have assumed that the amplitudes of the counterpropagating classical fields are equal, i.e. $\Omega_{s,\pm} \equiv \Omega_s$. In the limit when the excitations are mostly in spin-wave form, i.e. $\sin\theta_s \simeq 1$, and since $\sigma_{c,s;a} = -g\hat{E}_{s,\pm}/\Omega_s$, the polariton operators become

$$\Psi_{s,\pm} = \sqrt{2\pi n_z^s}\frac{g}{\Omega_s}\hat{E}_{s,\pm}. \tag{17}$$

Setting $\Psi_s = (\Psi_{s,+} + \Psi_{s,-})/2$ and $A_s = (\Psi_{s,+} - \Psi_{s,-})/2$ as the symmetric and antisymmetric combinations of the two polaritons, we derive the equations of motion for the polariton combinations Ψ_s, A_s:

$$\partial_t\Psi_s + \nu\partial_z A_s = -\pi\tan^2\theta_s\partial_t\Psi_s - i\frac{2\pi g^2}{\Delta_{ss}}\left(2\Psi_s^\dagger\Psi_s + A_s^\dagger A_s\right)\Psi_s - i\frac{2\pi g^2}{\Delta_{s\bar{s}}}\left(2\Psi_{\bar{s}}^\dagger\Psi_{\bar{s}} + A_{\bar{s}}^\dagger A_{\bar{s}}\right)\Psi_s + \text{noise},$$

$$\partial_t A_s + \nu\partial_z\Psi_s = -i\frac{2\pi g^2}{\Delta_s}n_z^s A_s - \frac{2\pi g^2}{\Delta_{ss}}\Psi_s^\dagger\Psi_s A_s + \text{noise}. \tag{18}$$

The noise terms in equation (18) account for the dissipative processes that take place during the evolution. Fortunately, for the dark-state polaritons under consideration, as long as the spontaneous emission rates Γ from the states $|c, s\rangle$ and $|d, s, s'\rangle$ are much less than the detunings $|\Delta_{ss'}|$, the losses in the time scales of interest are not significant and can thus be neglected as discussed in [26–30]. Assuming an optical depth of a few thousands and a large ratio of the density of atoms to the density of photons $n_z^s/n_{\text{ph}}^s \sim 10^4$, the antisymmetric combinations $A_\uparrow$ and $A_\downarrow$ can be adiabatically eliminated from the equations of motion for the polaritons and, moreover, nonlinear terms such as $\Psi_s^\dagger\Psi_s A_s$ and $A_s^\dagger A_s\Psi_s$ are negligible. In this regime, equation (18) simplifies to a nonlinear Schrödinger equation (19) for polaritons, which reads

$$i\partial_t\Psi_s = \frac{2\Delta_s\nu_s}{\Gamma_{1D}^s n_z^s}\partial_z^2\Psi_s + \frac{\Gamma_{1D}^s\nu_s}{\Delta_{ss}}\Psi_s^\dagger\Psi_s\Psi_s + \frac{\Gamma_{1D}^s\nu_s}{\Delta_{s\bar{s}}}\Psi_{\bar{s}}^\dagger\Psi_{\bar{s}}\Psi_s, \tag{19}$$

which is related to an effective two-component Lieb–Liniger model of polaritons,

$$H = \int dz \sum_s \left[\frac{1}{2m_s}\partial_z\Psi_s^\dagger(z)\partial_z\Psi_s(z) + \frac{\chi_s}{2}\rho_s^2(z)\right] + \int dz\chi_{\uparrow\downarrow}\rho_\uparrow(z)\rho_\downarrow(z). \tag{20}$$

Here $m_s = -\Gamma_{1D}^s n_z^s/(4\Delta_s\nu_s)$ is the effective mass for the sth polaritons with $\Gamma_{1D}^s = 4\pi g^2/\nu$ the spontaneous emission rate of a single atom into the waveguide modes and $\nu_s = \nu\Omega_s^2/(\pi g^2 n_z^s)$

---

[5] We would like to highlight here the relative simplicity of the above evolution equation compared to the one we considered in [30], where extra phase terms have to be involved due to the existence of two-atomic-species different frequencies on the incident quantum fields.

the group velocity of the propagating polaritons. The intraspecies repulsion is characterized by $\chi_s = \Gamma^s_{1D} \nu_s / \Delta_{ss}$ and the interspecies repulsion by $\chi_{\uparrow\downarrow} = \sum_{s=\uparrow,\downarrow} \Gamma^s_{1D} \nu_s / \Delta_{s\bar{s}}$.

To reach the spin–charge separation regime, we employ the mapping to a Luttinger liquid model described in the previous section. For this to be possible, we should first of all check the tunability of relevant parameters to the repulsive regime. This, in our case (see equation (19)), implies tuning $\Delta_s \Delta_{ss} < 0$, which leads to $m_s \chi_s > 0$. Similarly, $\Delta_\uparrow \Delta_\downarrow > 0$ forces the effective masses $m_\uparrow m_\downarrow > 0$ and $\Delta_{\uparrow\uparrow} \Delta_{\downarrow\downarrow} > 0$ tunes $\chi_\uparrow \chi_\downarrow > 0$. These conditions are satisfied by tuning the lasers such that $\Delta_\uparrow$ and $\Delta_\downarrow$ are negative (positive) while at the same time $\Delta_{\uparrow\uparrow}$ and $\Delta_{\downarrow\downarrow}$ are positive (negative).

In addition to the repulsive interaction regime, the separation condition equation (12) needs to be satisfied as well, which in our case means setting

$$\chi_\uparrow = \chi_\downarrow, \frac{\rho_{0,\uparrow}}{m_\uparrow} = \frac{\rho_{0,\downarrow}}{m_\downarrow}, \tag{21}$$

where the polariton density $\rho_{0,s}$ is equal to the photon density n^s_{ph}. The effective charge and spin densities are the sum and difference of the two-species polaritonic densities, which read

$$\rho_{\text{charge}} = \rho_\uparrow + \rho_\downarrow, \quad \rho_{\text{spin}} = \rho_\uparrow - \rho_\downarrow \tag{22}$$

with $\rho_s = \left(\rho_{0,s} - \frac{1}{\pi}\nabla\phi_s\right)\sum_m \exp\left[i2m\left(\pi\rho_{0,s}z - \phi_s\right)\right]$. Keeping only the lowest components with $m = 0, \pm 1$, the charge and spin density operators in the bosonic language can be represented as

$$\rho_{\text{charge}} = \rho_0 - \frac{\sqrt{2}}{\pi}\partial_z\phi_{\text{charge}} + 2\rho_0 \cos\left[2k_F z - \sqrt{2}\phi_{\text{charge}}\right]\cos\sqrt{2}\phi_{\text{spin}}, \tag{23}$$

$$\rho_{\text{spin}} = -\frac{\sqrt{2}}{\pi}\partial_z\phi_{\text{spin}} + 2\rho_0 \sin\left[2k_F z - \sqrt{2}\phi_{\text{charge}}\right]\sin\sqrt{2}\phi_{\text{spin}}. \tag{24}$$

Here the first term in ρ_{charge} is the average density $\rho_0 = \rho_{0,\uparrow} + \rho_{0,\downarrow}$. In our two-species photonic system, we set $\rho_{0,\uparrow} = \rho_{0,\downarrow} = \frac{1}{2}\rho_0$ for each polarization component. The second gradient terms in ρ_{charge} and ρ_{spin} are the density oscillations with zero momentum. The third term in ρ_{charge} and the second term in ρ_{spin} are the density fluctuations of the $2k_F$ components [37]. We label γ_s as the ratio of the interaction to the kinetic energies for each polariton species $\gamma_s = m_s \chi_s / \rho_{0,s}$. Combining the two separation conditions in equation (21) together, one gets $\gamma_\uparrow = \gamma_\downarrow$. For $\chi = \chi_s$ and $\gamma = \gamma_s$, the velocities and Luttinger parameters can be expressed as $u = \chi/\sqrt{\gamma}$ and $K = \pi/\sqrt{\gamma}$. As also demonstrated for a similar system albeit with one quantum field [29], γ here can also be tuned from zero to finite to extremely large, corresponding to non-, weak- and strong-correlated regimes, which implies a wide tunable range for u and K.

2.3. The probing of photonic spinons and holons

The typical detection of spin–charge separation can occur through dynamically probing the time evolution of a single excitation as in cold-atom proposals [12–15], or by measuring the corresponding single-particle spectral function as in condensed matter experiments [2–11]. In our case, we propose to extract the charge and spin velocities by measuring the Fourier transform of density–density correlations $D(\omega, q)$ for energy ω and momentum q. As was derived for
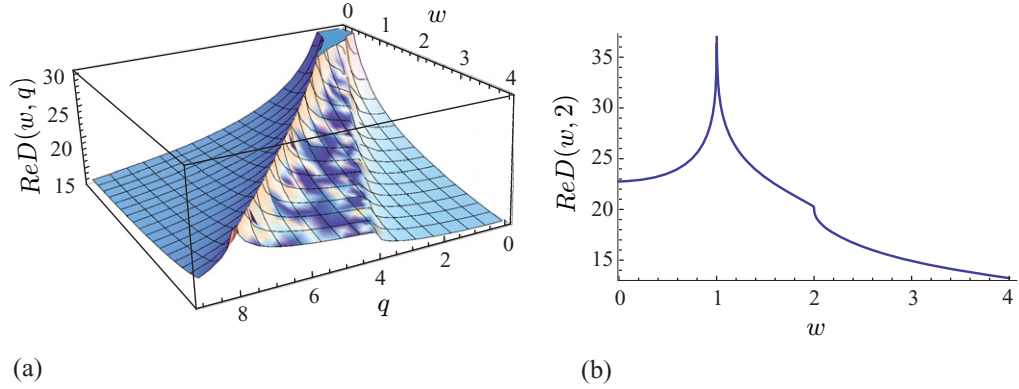
Figure 2. The Fourier transform of density–density correlations for our polaritonic system. It exhibits the characteristic splitting corresponding to the two different propagation velocities for the photonic spinons and holons, as calculated in [37]. The effective spin and charge velocities are $u_{\text{charge}} = 1$ and $u_{\text{spin}} = 0.5$ (normalized by $2\sqrt{\frac{2}{5}}u$), and the Luttinger parameters are $K_{\text{charge}} = 0.55$ and $K_{\text{spin}} = 1.1$. They translate in our case at optical depths of $OD = 2000$, 10 photons in each pulse initially, and single-atom cooperativity for each atomic species of 0.4. In (b) a cut of the 3D plot at quasi-momentum $q = 2$ is plotted to show the distinct two peaks corresponding to the spin and charge velocities. The cross density–density correlations are experimentally reconstructed via typical optical measurements on the correlated photon states as they exit the fiber.

the two-component system in [37], for the $2k_{\text{F}}$ component of the density operator $\rho_{2k_{\text{F}}} = 2\rho_0 \cos\left(2k_{\text{F}}z - \sqrt{2}\phi_{\text{charge}}\right) \cos\sqrt{2}\phi_{\text{spin}}$ (the last term of equation (23)), the Fourier transform $D(\omega, q)$ of the density–density operator $\left\langle T_\tau \rho_{2k_{\text{F}}}(z, \tau) \rho_{2k_{\text{F}}}(0, 0)\right\rangle$ is given by

$$D(\omega, q) = -\frac{4\pi\rho_0^2 \left(\frac{\alpha}{2}\right)^{K_{\text{charge}}+K_{\text{spin}}} \Gamma\left(1 - K_{\text{charge}}/2 - K_{\text{spin}}/2\right)}{\Gamma\left(K_{\text{charge}}/2 + K_{\text{spin}}/2\right)} \times \left|\omega^2 - u_{\text{spin}}^2 q^2\right|^{K_{\text{charge}}/2 + K_{\text{spin}}/2 - 1} u_{\text{spin}}^{1 - K_{\text{charge}} - K_{\text{spin}}}$$

$$\times \exp\left[-i\pi\left(\frac{K_{\text{charge}}+K_{\text{spin}}}{2} - 1\right)\Theta\left(\omega^2 - u_{\text{spin}}^2 q^2\right)\right] \times F_1\left(\frac{K_{\text{charge}}}{2}, \frac{K_{\text{charge}}+K_{\text{spin}}-1}{2},\right.$$

$$\left. 1 - \frac{K_{\text{charge}}+K_{\text{spin}}}{2}, \frac{K_{\text{charge}}+K_{\text{spin}}}{2}; 1 - \frac{u_{\text{charge}}^2}{u_{\text{spin}}^2}, 1 - \frac{\omega^2 - u_{\text{charge}}^2 q^2}{\omega^2 - u_{\text{spin}}^2 q^2}\right), \quad (25)$$

where Γ is the gamma function, Θ is the step function, F_1 is Appell's hypergeometric function and α is a short-distance cutoff. $D(\omega, q)$ depends on the velocity ω/q and should exhibit two peaks centered around $u_{\text{charge}}q$ and $u_{\text{spin}}q$ [2–5]. In our photonic system, probing of the spinon and holon branches can be done by measuring the correlation functions of densities of the fields as they exit, for a specific quasi-momenta q. For a clear distinction between the two effective spin and charge peaks, we should set our optical detectors around $q = 2\pi/z_0$, i.e. z_0 apart (z_0 here corresponds to roughly the length of the fiber). To give an illustration of the expected behavior, $D(\omega, q)$ in units of $\rho_0^2\alpha$ is plotted in figure 2 with the intra- and interspecies repulsion

ratio $\chi_{\uparrow\downarrow}/\chi = 0.6$, which in turn tunes the charge and spin velocities to

$$u_{\text{charge}} = 2u_{\text{spin}} = u\sqrt{1 + \chi_{\uparrow\downarrow}/\chi} = 2\sqrt{\frac{2}{5}}u, \tag{26}$$

and the Luttinger parameters $K_{\text{charge}} = \frac{1}{2}K_{\text{spin}} = \frac{1}{2}\sqrt{\frac{5}{2}}K$. We choose $u_{\text{charge}} = 1$, $u_{\text{spin}} = 0.5$ and $K_{\text{charge}} = 0.55$, $K_{\text{spin}} = 1.1$ via tuning u and K which require $\gamma \sim 20$. This as shown in [29] is achieved at optical depths OD $= 2000$ and roughly $N_{\text{ph}}^{\uparrow,\downarrow} = 10$ photons initially in each pulse and single-atom co-operativity of $\eta = 0.4$.[6] These values are for the moment out of the current experimental range where optical depths of a few hundreds have been achieved, but should not be out of the question in the near to mid-term future [31, 32, 38]. In calculating the optical interaction parameters appearing in the Hamiltonian equation (20), we have taken into account both the linear and nonlinear loss mechanisms as laid out in [29].

3. Conclusion

We have described in detail a strongly correlated photonic scheme to simulate a purely fermionic effect, namely spin–charge separation. In more detail, we have shown that polarized photons interacting with a cold atomic ensemble can be made to obey two-component Lieb–Liniger physics and even behave like a quantum Luttinger liquid. The relevant interactions exhibit the necessary tunability for steering the photons to the effective spin–charge separation regime. Efficient observations of the characteristic features of the separation using standard quantum optical methods should be feasible based on correlations measurements of the outgoing photons which here carry opposite polarizations. The current proposal is different from a similar scheme proposed earlier by some of us, where two species of atoms were coupled to two quantum fields of two different frequencies but of the same polarization [30]. Here, a single species of atoms is shown to be sufficient to induce the required intra- and interspecies interactions, which combined with the easier detection of the polarized output states renders this approach more feasible.

Acknowledgments

References

[1] Lieb E H and Liniger W 1963 *Phys. Rev.* **130** 1605
[2] Giamarchi T 2004 *Quantum Physics in One Dimension* (Oxford: Oxford University Press)
[3] Girardeau M 1960 *J. Math. Phys.* **1** 516–23
[4] Girardeau M 1965 *Phys. Rev.* **139** B500
[5] Paredes B *et al* 2004 *Nature* **429** 277–81
[6] Kim C *et al* 1996 *Phys. Rev. Lett.* **77** 4054–7
[7] Segovia P, Purdie D, Hengsberger M and Baer Y 1999 *Nature* **402** 504–7

---

[6] Cooperativity here is the ratio of spontaneous emission into the waveguide to the total spontaneous emission.

IOP Institute of Physics · DEUTSCHE PHYSIKALISCHE GESELLSCHAFT

 [8] Lorenz T, Hofmann M, Grüninger M, Freimuth A, Uhrig G S, Dumm M and Dressel M 2002 *Nature* **418** 614–7

 [9] Auslaender O M *et al* 2005 *Science* **308** 88–92

[10] Kim B J *et al* 2006 *Nature Phys.* **2** 397–401

[11] Jompol Y *et al* 2009 *Science* **325** 597–601

[12] Recati A, Fedichev P O, Zwerger W and Zoller P 2003 *Phys. Rev. Lett.* **90** 020401

[13] Kecke L, Grabert H and Hausler W 2005 *Phys. Rev. Lett.* **94** 176802

[14] Kollath C, Schollwöck U and Zwerger W 2005 *Phys. Rev. Lett.* **95** 176401

[15] Kleine A, Kollath C, McCulloch I P, Giamarchi T and Schollwöck U 2008 *Phys. Rev.* A **77** 013607

[16] Angelakis D G, Santos M F, Yannopapas V and Ekert A 2007 *Phys. Lett.* A **362** 377–80

[17] Angelakis D G, Santos M F and Bose S 2007 *Phys. Rev.* A **76** 031805

[18] Hartmann M J, Brandão F G S L and Plenio M B 2006 *Nature Phys.* **2** 849–55

[19] Greentree A D, Tahan C, Cole J H and Hollenberg L C L 2006 *Nature Phys.* **2** 856–61

[20] Rossini D and Fazio R 2007 *Phys. Rev. Lett.* **99** 186401

[21] Na N, Utsunomiya S, Tian L and Yamamoto Y 2008 *Phys. Rev.* A **77** 031803

[22] Aichhorn M, Hohenadler M, Tahan C and Littlewood P B 2008 *Phys. Rev. Lett.* **100** 216401

[23] Gerace D, Türeci H E, Imamoglu A, Giovannetti V and Fazio R 2009 *Nature Phys.* **5** 281–4

[24] Carusotto I *et al* 2009 *Phys. Rev. Lett.* **103** 033601

[25] Angelakis D G, Bose S and Mancini S 2009 *Eur. Phys. Lett.* **85** 20007

[26] Fleischhauer M and Lukin M D 2000 *Phys. Rev. Lett.* **84** 5094–7

[27] Bajcsy M, Zibrov A S and Lukin M D 2003 *Nature* **426** 638–41

[28] Bajcsy M *et al* 2009 *Phys. Rev. Lett.* **102** 203902

[29] Chang D E *et al* 2008 *Nature Phys.* **4** 884–9

[30] Angelakis D G, Huo M-X, Kyoseva E and Kwek L C 2011 *Phys. Rev. Lett.* **106** 153601

[31] Nayak K P *et al* 2007 *Opt. Express* **15** 5431–8

[32] Vetsch E, Reitz D, Sague G, Schmidt R, Dawkins S T and Rauschenbeutel A 2010 *Phys. Rev. Lett.* **104** 203603

[33] Ghosh S, Sharping J E, Ouzounov D G and Gaeta A L 2005 *Phys. Rev. Lett.* **94** 093902

[34] Takekoshi T and Knize R J 2007 *Phys. Rev. Lett.* **98** 210404

[35] Christensen C A *et al* 2008 *Phys. Rev.* A **78** 033429

[36] Vorrath S, Möller S A, Windpassinger P, Bongs K and Sengstock K 2010 *New J. Phys.* **12** 123015

[37] Iucci A, Fiete G A and Giamarch T 2007 *Phys. Rev.* B **75** 205116

[38] Bajcsy M *et al* 2011 *Phys. Rev.* A **83** 063830